



OPEN ACCESS

EDITED BY

Chenhe Su,
Wistar Institute, United States

REVIEWED BY

Xiaochuan Liu,
University of California, Riverside,
United States
Huibin Yu,
Yale University, United States
Jun Yan,
Fudan University, China

*CORRESPONDENCE

Junjiang Fu
fujunjiang@swmu.edu.cn
Dabing Li
lidabing2018@163.com
Xiaoyan Liu
405071800@qq.com

[†]These authors have contributed
equally to this work

SPECIALTY SECTION

This article was submitted to
Viral Immunology,
a section of the journal
Frontiers in Immunology

RECEIVED 01 June 2022

ACCEPTED 26 August 2022

PUBLISHED 13 September 2022

CITATION

Cheng J, Fu J, Tan Q, Liu Z, Guo K,
Zhang L, He J, Zhou B, Liu X, Li D and
Fu J (2022) The regulation of ISG20
expression on SARS-CoV-2 infection
in cancer patients and
healthy individuals.
Front. Immunol. 13:958898.
doi: 10.3389/fimmu.2022.958898

COPYRIGHT

© 2022 Cheng, Fu, Tan, Liu, Guo,
Zhang, He, Zhou, Liu, Li and Fu. This is
an open-access article distributed under
the terms of the [Creative Commons
Attribution License \(CC BY\)](https://creativecommons.org/licenses/by/4.0/). The use,
distribution or reproduction in other
forums is permitted, provided the
original author(s) and the copyright
owner(s) are credited and that the
original publication in this journal is
cited, in accordance with accepted
academic practice. No use,
distribution or reproduction is
permitted which does not comply with
these terms.

The regulation of ISG20 expression on SARS-CoV-2 infection in cancer patients and healthy individuals

Jingliang Cheng^{1†}, Jiewen Fu^{1†}, Qi Tan^{1†}, Zhiying Liu^{1†},
Kan Guo¹, Lianmei Zhang^{1,2}, Jiayue He¹, Baixu Zhou^{1,3},
Xiaoyan Liu^{1*}, Dabing Li^{1,4*} and Junjiang Fu^{1*}

¹Key Laboratory of Epigenetics and Oncology, The Research Center for Preclinical Medicine, Southwest Medical University, Luzhou, China, ²Department of Pathology, The Affiliated Huaian No. 1 People's Hospital of Nanjing Medical University, Huai'an, China, ³Department of Gynecology and Obstetrics, Guangdong Women and Children Hospital, Guangzhou, China, ⁴Basic Medical School, Southwest Medical University, Luzhou, China

ISG20 inhibits viruses such as SARS-CoV-2 invasion; however, details of its expression and regulation with viral susceptibility remain to be elucidated. The present study analyzed ISG20 expression, isoform information, survival rate, methylation patterns, immune cell infiltration, and COVID-19 outcomes in healthy and cancerous individuals. Cordycepin (CD) and N6, N6-dimethyladenosine (m⁶₂A) were used to treat cancer cells for ISG20 expression. We revealed that *ISG20* mRNA expression was primarily located in the bone marrow and lymphoid tissues. Interestingly, its expression was significantly increased in 11 different types of cancer, indicating that cancer patients may be less vulnerable to SARS-CoV-2 infection. Among them, higher expression of ISG20 was associated with a long OS in CESC and SKCM, suggesting that ISG20 may be a good marker for both viral prevention and cancer progress. *ISG20* promoter methylation was significantly lower in BLCA, READ, and THCA tumor tissues than in the matched normal tissues, while higher in BRCA, LUSC, KIRC, and PAAD. Hypermethylation of *ISG20* in KIRC and PAAD tumor tissues was correlated with higher expression of *ISG20*, suggesting that methylation of *ISG20* may not underlie its overexpression. Furthermore, ISG20 expression was significantly correlated with immune infiltration levels, including immune lymphocytes, chemokine, receptors, immunoinhibitors, immunostimulators, and MHC molecules in pan-cancer. STAD exhibited the highest degree of *ISG20* mutations; the median progression-free survival time in months for the unaltered group was 61.84, while it was 81.01 in the mutant group. Isoforms ISG20-001 and ISG20-009 showed the same RNase_T domain structure, demonstrating the functional roles in tumorigenesis and SARS-CoV-2 invasion inhibition in cancer patients. Moreover, CD and m⁶₂A increase ISG20 expression in various cancer cell lines, implying the antiviral/anti-SARS-CoV-2 therapeutic potential. Altogether, this study highlighted the value of combating cancer by targeting ISG20 during the COVID-19 pandemic, and small molecules extracted from traditional Chinese medicines, such as CD,

may have potential as anti-SARS-CoV-2 and anticancer agents by promoting ISG20 expression.

KEYWORDS

ISG20 expression, cancer, SARS-CoV-2, cordycepin (CD), N6, N6-dimethyladenosine (m⁶2A)

1 Introduction

Interferon stimulated exonuclease gene 20 (ISG20, OMIM: 604533) aliases HEM45, CD25, Promyelocytic leukemia nuclear body-associated protein ISG20, interferon-stimulated exonuclease gene 20 kDa, interferon-stimulated gene 20 KDa protein, estrogen-regulated transcript 45 protein, and EC 3.1.13.1. ISG20 cytogenetic locates on chromosome 15q26.1 and genomic coordinates (GRCh38) between 15:88,635,631 and 88,656,4820 was first isolated by Gongora et al. in 1997 as a cDNA encoding an interferon-induced protein, called ISG20, by screening an IFN-treated Daudi cell cDNA library (1). Pentecost (1998) identified a cDNA that encoded a 181-amino acid protein with a predicted molecular weight of 20,363 Da; the expression of *ISG20* mRNA was increased in response to estrogen in estrogen receptor-expressing cells in the presence of cycloheximide (2).

ISG20 is predicted to exhibit a broad spectrum of antiviral activity, including hepatitis A virus (HAV), hepatitis B virus (HBV), hepatitis C virus (HCV), Influenza A virus (IAV), and yellow fever virus (YFV) in an exonuclease-dependent manner, through the degradation of viral RNA as a 3'-5'-exoribonuclease (3, 4). Additional antiviral mechanisms by ISG20 include translational inhibition of viral RNA and non-self RNAs and degradation of deaminated viral DNA (3, 5–7). ISG20 has also been reported to inhibit the replication of bluetongue virus (BTV) in ovine (8) and to inhibit the proliferation of pseudorabies virus (PRV) (9, 10). Furthermore, a recent study suggested that ISG20 can degrade SARS-CoV-2 (severe acute respiratory syndrome coronavirus 2) sub-replicon RNA through exonuclease activity (11). The SARS-CoV-2 is the pathogen underlying the current COVID-19 (coronavirus disease 2019) pandemic, leading to more than 596 million positive cases and 6 million deaths worldwide (<https://coronavirus.jhu.edu/>).

Similarly, ISG20 acts as a SARS-CoV-2 RNase and is critical in inhibiting the SARS-CoV-2 replicon in host cells. Therefore, the expression and distribution of ISG20 may explain the differences in COVID-19 severity after the SARS-CoV-2 invasion. Cellular and humoral immunity participate in the prevention of viral invasion, and the pathological process of COVID-19 is likely correlated with the dysregulation of the

immune response, particularly of T cells. Targeting ISG20 may thus be a potential therapeutic strategy for managing SARS-CoV-2 infection.

A large body of evidence has indicated the effect of COVID-19 on the clinical outcomes of cancer patients. According to cohort studies of COVID-19 on the Cancer Consortium and systematic reviews, patients with cancer and COVID-19 exhibit increased mortality rates (12–15). Thus, increased attention should be paid to patients with cancer during the COVID-19 pandemic.

Herein, we performed comprehensive and integrative profiling of ISG20 expression in healthy individuals and patients using a pan-cancer dataset using genomic, transcriptomic, and epigenomic data. The relationships between the expression of ISG20 and immune cell infiltration were investigated. These results may highlight the significance of SARS-CoV-2 infection in patients with different cancer types and the potential therapeutic value of using small molecules such as cordycepin (CD) and N6, N6-dimethyladenosine (m⁶2A) in managing SARS-CoV-2 infection.

2 Materials and methods

2.1 Online databases

ISG20 homologs in humans from GenBank (Protein: NP_001290162.2, Gene: NM_001303233.2) and others were obtained from NCBI (National Center for Biotechnology Information) (<https://www.ncbi.nlm.nih.gov/homologene/31081>) (16, 17). Data on gene and protein expression levels of ISG20 in the normal and cancerous tissues (<https://www.proteinatlas.org/ENSG00000172183-ISG20/tissue>), in different types of immune cells (RNA) (<https://www.proteinatlas.org/ENSG00000172183-ISG20/immune+cell>), in single cells (<https://www.proteinatlas.org/ENSG00000172183-ISG20/single+cell+type>), and brain tissues (<https://www.proteinatlas.org/ENSG00000172183-ISG20/brain>) were obtained from the Human Protein Atlas (HPA) (18, 19). *ISG20* expression in different types of cancer tissues and the corresponding normal tissues, isoform, distribution, and domain structures were

analyzed using GEPIA 2 (gene expression profiling interactive analysis 2) (<http://gepia2.cancer-pku.cn/#analysis>) and (<http://gepia2.cancer-pku.cn/#isoform>) (20, 21). DNA methylation analysis of the *ISG20* promoter was performed using DNMIVD (DNA methylation interactive visualization database) (http://119.3.41.228/dnmivd/query_gene/?cancer=pancancer&gene=ISG20) (22). Data on *ISG20* mutations were obtained from cBioPortal for cancer genomics (https://www.cbioportal.org/results/cancerTypesSummary?case_set_id=all&gene_list=ISG20&cancer_study_list=5c8a7d55e4b046111fee2296) (23). Survival analysis of *ISG20* expressions was performed using GEPIA 2, DNMIVD, and cBioPortal. Analysis of the relationships between the abundance of tumor-infiltrating lymphocytes (TILs) and expression was performed using TISIDB (an integrated repository portal for tumor-immune system interactions) (<http://cis.hku.hk/TISIDB/browse.php?gene=ISG20>) (24).

2.2 Immunohistochemistry analysis

Immunohistochemistry (IHC) in formalin-fixed, paraffin-embedded breast cancer tissue sections from Chinese patients was performed as described previously (17, 25–27). The *ISG20* antibody (C-12, cat #: sc-514979) for IHC and western blotting was purchased from Santa Cruz Biotechnology, Inc., USA. For details, 5 μ m deparaffinized and rehydrated sections were incubated in 10 μ M sodium citrate buffer at 95°C for 12 min for antigen retrieval, and treated with 3% hydrogen peroxide. Then blocking with 5% bovine serum albumin (BSA). Primary *ISG20* antibody (1:50 dilution) was applied overnight and then incubated with appropriate biotin-conjugated secondary antibodies (SP-9000, ZSGB-Bio, CN) for 60 min at 25°C. Immunostaining signals were visualized by the Streptavidin-conjugated horseradish peroxidase (HRP) and 3,3'-diaminobenzidine (DAB) (ZLI-9017, ZSGB-Bio, CN). Slides were counterstained with hematoxylin, dehydrated, and mounted.

2.3 Cell culture

Cancer cell lines A549, H1975, HepG2, 22RV1, PC3, BT549, MDA-MB-231, and HeLa were obtained from ATCC (American Type Culture Collection), and cultured in DMEM or RPM1640 supplemented with 10% serum and 1% penicillin-streptomycin (Gibco; Thermo Fisher Scientific, Inc.) in 12-well plates. CD (Cat #: A0682) was obtained from Chengdu Must Bio-Technology Co. Ltd (Chengdu, Sichuan, China), m⁶2A (CAS #: 2620-62-4) from BOC Sciences (Shirley, NY, USA), and uridine-5'-monophosphate (UMP, CAS #: 58-97-9) from Shanghai Aladdin Biochemical Technology company (Shanghai, China). Total RNA and protein were extracted after UMP, CD, or m⁶2A

treatment with the indicated concentrations for 24 h. The cells were lysed using EBC buffer (20 mM Tris-HCl, pH 8.0, 125 mM NaCl, 2 mM EDTA, and 0.5% NP-40) supplemented with a protease and phosphatase inhibitor cocktail. The harvested protein was stored at -20°C until required.

2.4 Western blotting

SDS-PAGE was used for western blotting. After electrophoresis at 100v for 100 min, the proteins were transferred to membranes at 100v for approximately 90 min. Then the membranes were blocked with fresh 5% fat-free milk at room temperature for 2 h. Primary antibodies against *ISG20*, β -actin, or HSP90 were incubated in the fresh 2% fat-free milk at 4°C overnight. The following day, membranes were washed three times with TBST (Tris-buffered saline containing 0.1% Tween20) for 15 min each time, and the blots were incubated with an anti-mouse HRP secondary antibody (1:5000 dilution) in 2% fat-free milk for a further 2 h. Subsequently, the membranes were three times as above. The protocol for western blot in breast cancer tissues and its matched healthy tissues from Chinese breast cancer patients was described previously (25, 26). All experiments were repeated three times.

2.5 Semi-quantitative reverse transcription-polymerase chain reaction

The harvested total RNA was reverse transcribed into cDNA. The sequences of the primers targeting *ISG20* (NM_001303233.2) were: RT-*ISG20*-5: 5'-ctccaggcactgaaagagg-3' (forward primer), RT-*ISG20*-3: 5'-aagccgaagccttagtcc-3' (reverse primer). The expected product size was 309 bp. These primers would expect to detect isoforms *ISG20*-001 and *ISG20*-009, two main isoforms for *ISG20* in Figure 5C. *ACTB* was used as the internal control. The sequences of the primers *ACTB* were: RT-*ACTB*-5: 5'-CTCTTCCAGCCTTCCTTCCT-3' (forward primer), RT-*ACTB*-3: 5'-CACCTTCACCGTTCCAGTTT-3' (reverse primer). The expected product size was 510 bp. Semi-quantitative RT-PCR was performed as described previously (28). All experiments were repeated three times.

2.6 Statistical analysis

To compare the expression of *ISG20* in pan-cancer and in the matched healthy tissues, $|\log_2FC|$ values were used and log-rank $P < 0.05$ was considered statistically significant. For comparison of the methylation of the *ISG20* promoter region in cancer tissues and the corresponding healthy tissues, a student's t-test was used, and P -value < 0.05 was considered significant.

3 Results

3.1 Expression of ISG20 in normal tissues

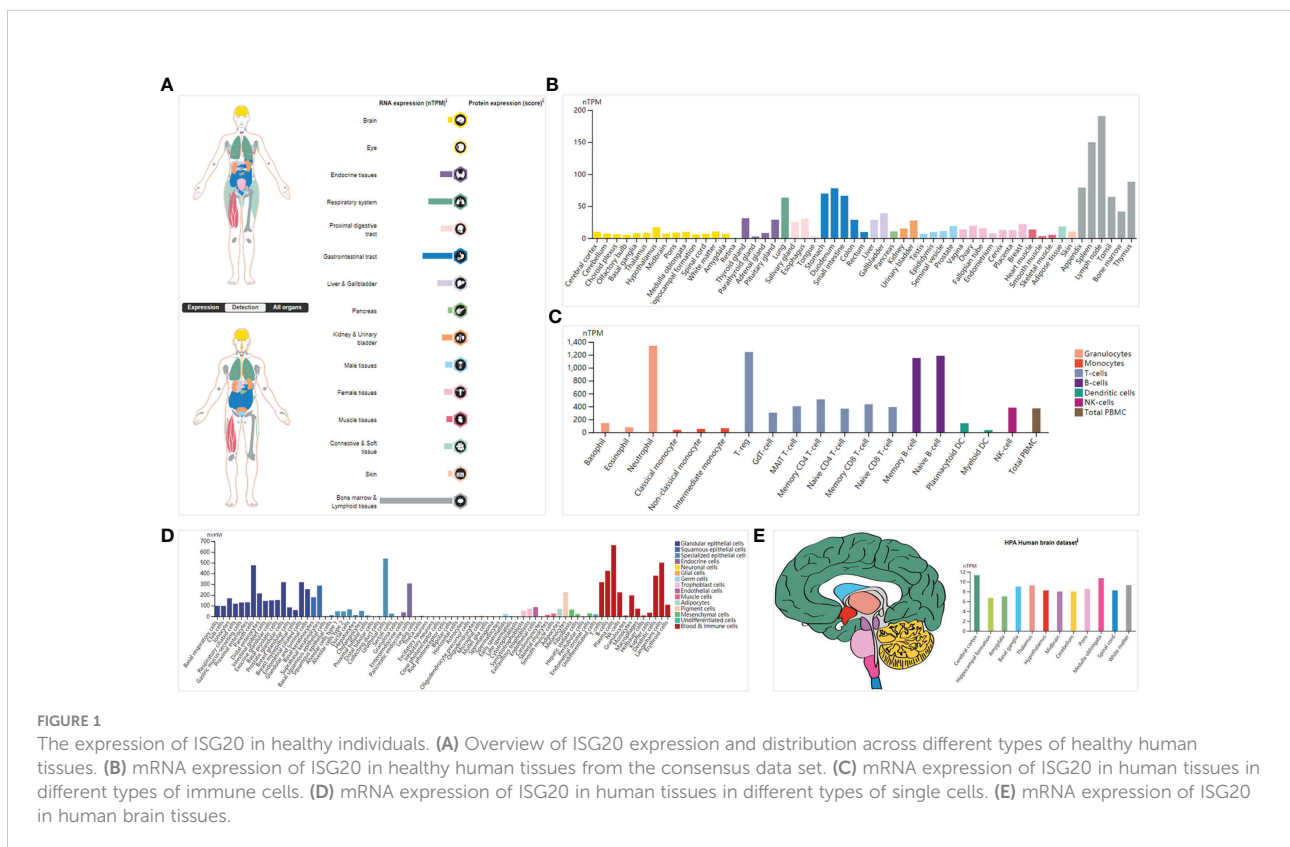
The transcriptional data on *ISG20* expression in human organs and tissues is presented in **Figure 1A**; *ISG20* mRNA was mainly located in the bone marrow and lymphoid tissues, followed by the gastrointestinal tract, respiratory system, liver and gallbladder, endocrine tissues, and kidney and urinary bladder, with no expression in the eyes. High expression of *ISG20* in the respiratory system (lung, 63.3nTPM) demonstrated its antiviral role in the lungs. The expression of *ISG20* mRNA was further validated in the consensus data set (**Figure 1B**). In agreement with the above results, the top nine tissues/organs for *ISG20* mRNA expressions in this consensus dataset were the lymph node, spleen, thymus, appendix, and tonsils (they are bone marrow and lymphoid tissues), stomach, duodenum, and small intestine (they are gastrointestinal tract), and lungs (**Figure 1B**). Then, the mRNA expression levels of *ISG20* were examined in human tissues of immune cells, single cell types, and the brain. The results of 18 immune cell types and total peripheral blood mononuclear cells (PBMCs) indicated that *ISG20* mRNA expression was very high in neutrophils, T-reg, memory B-cells, and naive B-cells (all >1,150 nTPM) (**Figure 1C**). The *ISG20* mRNA expression in single-cell-type specificity indicated it was predominantly expressed in the

plasma cells (663.4 nTPM), Langerhans cells (500.2 nTPM), B-cells (424.2 nTPM), dendritic cells (378.8 nTPM), T-cells (318.4 nTPM), urothelial cells (538.6 nTPM), and paneth cells (476.1 nTPM) (**Figure 1D**). The mRNA expression levels of *ISG20* in the brain were very low but remained detectable, with the highest levels observed in the cerebral cortex (11.3 nTPM) (**Figure 1E**). The *ISG20* expression was unavailable (NA) in human blood cells from HPA.

Next, we conducted IHC of breast cancer tissues; representative results are shown in **Figures 2A–F**. *ISG20* staining showed high expression in the cytoplasm and membranes in the breast tissues (**Figures 2A, B**) and breast cancer tissues (**Figures 2, D**). *ISG20* was primarily located in the cytoplasm and membrane (highest in the cytoplasm), indicating its role in viral prevention. As a control, we also showed IHC images of breast tissues and breast cancer tissues without antibodies, respectively, in **Figures 2E, F**.

3.2 *ISG20* expression is increased in cancer tissues compared with the corresponding normal tissues

Increasing evidence has shown that cancer patients are more vulnerable to SARS-Cov-2. As an enigmatic antiviral factor, it is important to know the expression levels of *ISG20* in cancer



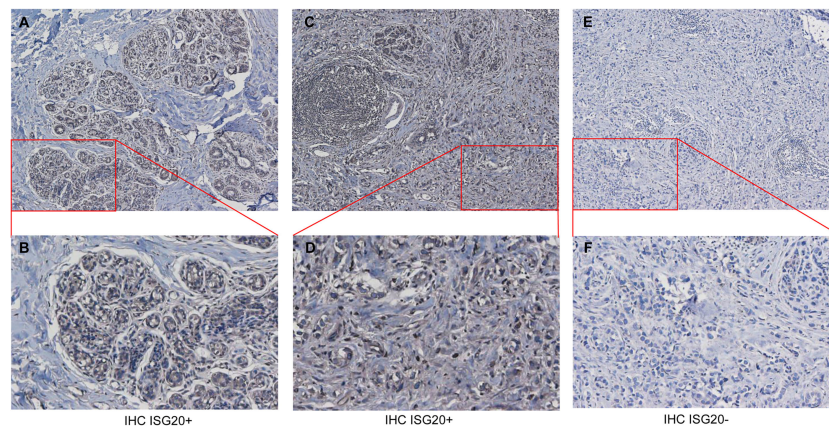


FIGURE 2

Immunohistochemistry (IHC) analysis of ISG20 expression healthy and cancer tissues from breast cancer patients. (A, B) IHC analysis of ISG20 in breast tissues. (C, D) IHC analysis of ISG20 in breast cancer tissues. (E, F) Control IHC of breast tissues without antibody. Panels (B, D) show enlarged insets from (A, C), respectively.

tissues compared with corresponding healthy tissues. Surprisingly, *ISG20* mRNA expression was significantly increased in eleven types of cancer, including ACC (adrenocortical carcinoma), CESC (cervical squamous cell carcinoma and endocervical), DLBC (lymphoid neoplasm diffuse large B-cell lymphoma), GBM (glioblastoma multiforme), KIRC (Kidney renal clear cell carcinoma), LIHC (liver hepatocellular carcinoma), KIRP (kidney renal papillary cell carcinoma), PAAD (pancreatic adenocarcinoma), SKCM (skin cutaneous melanoma), TGCT (testicular germ cell tumors), and UCEC (uterine corpus endometrial carcinoma) (Figures 3A, B) compared with the matching normal tissue. Thus, high *ISG20* expression in cancer may prevent viral invasion in these cancer patients.

To further validate the expression results, samples of breast cancer tissues and their matched healthy tissues were selected for collection and western blot since *ISG20* levels are increased even though not significantly (Supplementary Figure 1A). It is also easy for us to collect breast tumor tissues. After western blot and the results were presented in Supplementary Figure 1B, *ISG20* protein levels were increased significantly in 6 of 10 samples/patients (60%) of cancer tissues compared with the matched healthy tissues (Supplementary Figure 1B). These results validated the mRNA results from the TCGA database for BRCA (breast invasive carcinoma) patients.

3.3 The prognostic value of *ISG20* in pan-cancer

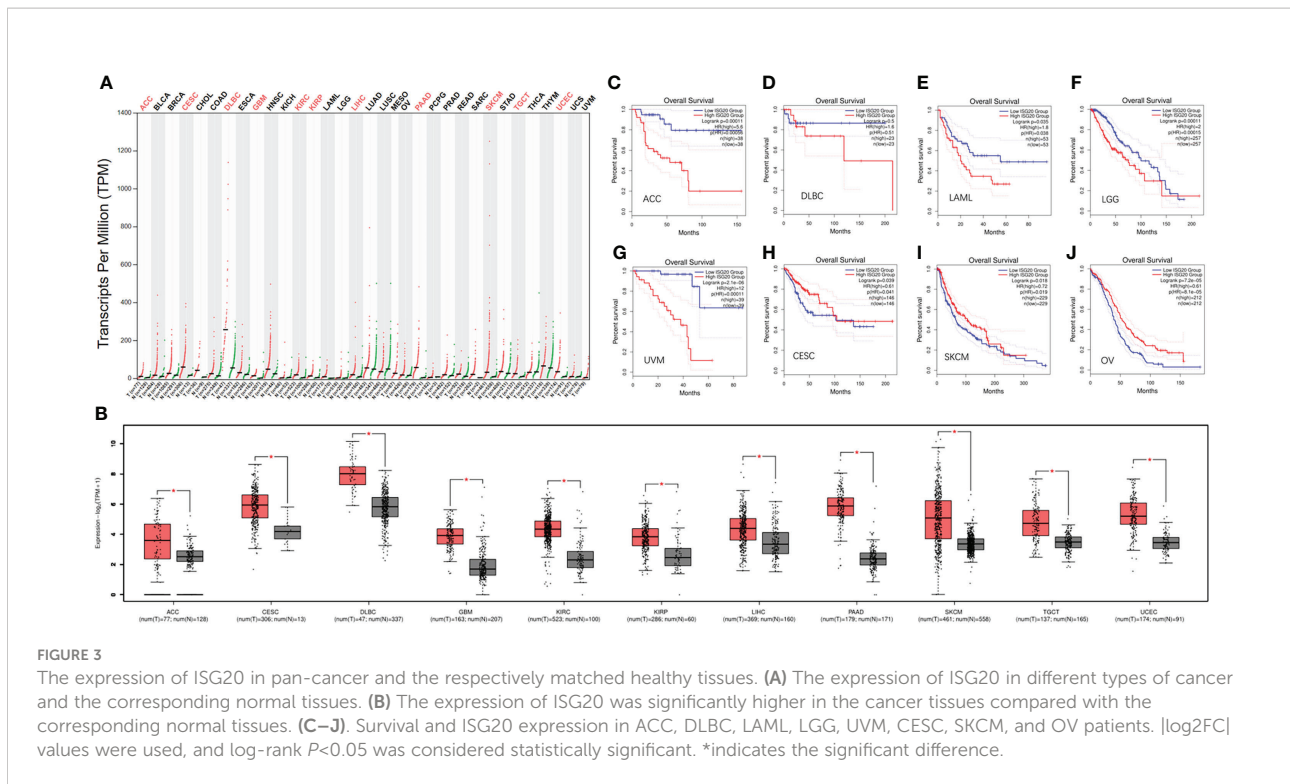
Further exploration of the prognostic value of *ISG20* revealed that higher expression was associated with a shorter OS in ACC, DLBC, LAML (acute myeloid leukemia), LGG

(lower grade glioma), and UVM (uveal melanoma) (Figures 3C–G), but with a long OS in CESC, OV (ovarian serous cystadenocarcinoma), and SKCM (Figures 3H–J). It was reported that *ISG20* overexpression suppressed the proliferation, migration, and invasion *in vitro* and the growth of xenograft tumors *in vivo* in ovarian cancer (29), and it may be associated with a long OS in OV patients.

High expression of *ISG20* in CESC and SKCM was associated with a longer OS, suggesting that *ISG20* may be a good marker. However, high expression of *ISG20* in ACC and DLBC was associated with a shorter OS, suggesting that *ISG20* may be a marker of unfavorable outcomes in these types of cancer. Together, *ISG20* may serve as a double-edged sword in viral prevention and cancer progression in certain types of cancer.

3.4 Methylation of the *ISG20* promoter region in cancer and the matched normal tissues

DNA methylation can regulate gene expression. We'd like to know whether *ISG20* expression changes are due to methylation modification. By analyzing the DNMIVD database, we found that *ISG20* promoter methylation was significantly lower in BLCA, READ, and THCA tumor tissues compared to the matching normal tissue (Figures 4A–C), while higher in BRCA, LUSC, KIRC, and PAAD (Figures 4D–G). Hypermethylation of *ISG20* in KIRC and PAAD tumor tissues was correlated with the higher expression, suggesting that methylation of *ISG20* may not be the cause of overexpression. Thus, other mechanisms may be involved in regulating *ISG20* expression.



3.5 Expression distribution, utilization, and structure of ISG20 in pan-cancer, and conservation across different species

Different ACE2 isoforms have differential roles in host susceptibility to SARS-CoV-2 entry (30, 31). We analyzed ISG20 isoform prevalence and structures in pan-cancer and found 11 isoforms that exhibited differential expression levels (Figure 5A). Except for very low or no expression of isoforms ENST00000558992.1 (ISG20-010), ENST00000558942.5 (ISG20-003), and ENST00000558236.1 (ISG20-011), the remaining eight ISG20 isoforms were detectable in all cancers.

The utilization of isoform ENST00000560741.5 (ISG20-009) was the highest across all 31 cancer types, followed by ENST00000559876.1 (ISG20-006); others showed very low or no utilization (Figure 5B). The genomic structures of ISG20 isoforms in pan-cancer are shown in Figure 5C. The isoforms ENST00000306072.9 (ISG20-001) and ENST00000560741.5 (ISG20-009) showed the same structure consisting of 181 amino acids with an RNase_T domain as reported previously; isoforms ENST00000559876.1 (ISG20-006) with 155 amino acids and ENST00000379224.9 (ISG20-008) with 87 amino acids, both possessed a truncated RNase_T domain (Figure 5C), demonstrating the functional role of ISG20-001 and ISG20-009 in tumorigenesis and SARS-CoV-2 invasion inhibition in cancer patients.

In addition, the ISG20 protein showed a highly conserved sequence across different species, including humans,

chimpanzee, Rhesus monkey, cows, dog, mice, and rats (Figure 5D), suggesting that ISG20 may possess a similar potential function in inhibiting viral infection in other species (8). Indeed, ISG20 was also reported to inhibit the bluetongue virus (BTV) replication in sheep (8).

3.6 Mutation profiles of ISG20 in pan-cancer

Gene mutations can cause cancer, recurrence, and/or therapeutic resistance. By analyzing the ISG20 mutation profile in 32 types of cancer based on data obtained from TCGA, we found that STAD (stomach adenocarcinoma) had the highest mutational frequency, with 3.64% of 440 cases possessing a mutation, followed by SARC (3.53% of 255 cases), whereas BLGG (brain lower grade glioma) had the lowest frequency of mutations (0.19% of 514 cases) (Figure 6A). No ISG20 mutations were found in the other 11 types of cancer shown in Figure 6A. The detailed landscape of mutations shows the presence of missense mutations, truncations, and SV/fusions in the ISG20 gene, with missense mutations being the most common (Figure 6B).

To further explore the resulting prognostic value, we analyzed the survival correlation between ISG20 mutant groups and unaltered groups in cancer. However, no significant difference was observed ($P=0.0679$), and the median number of months of progression-free survival for the unaltered

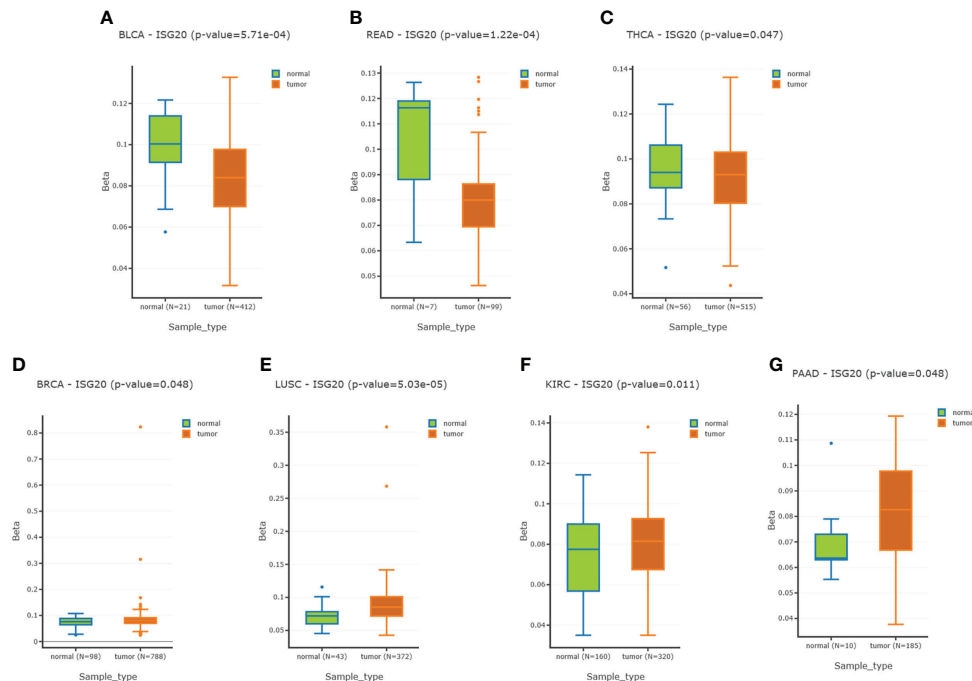


FIGURE 4

Methylation of the ISG20 promoter region in cancer tissues and the corresponding healthy tissues. (A–C). Methylation of the ISG20 promoter region in cancer tissues was significantly lower than in the corresponding healthy tissues for BLCA, READ, and THCA, respectively. (D–G). Methylation of the ISG20 promoter region in cancer tissues was significantly higher than in the corresponding healthy tissues for BRCA, LUSC, KIRC, and PAAD, respectively. The student's t-test was used and P -value < 0.05 was considered significant.

group was 61.84 months (56.05–66.11, 95% CI), while in the mutant groups, it increased to 81.01 months (48.89–NA, 95% CI) (Figure 6C).

3.7 Association analysis of *ISG20* expression with the tumor-immune system in pan-cancer

Due to the indispensability of antiviral processes and anti-tumor responses of the immune system, the correlation between *ISG20* expression and immune infiltration levels in pan-cancer was analyzed in the TISDB database. We also found significant correlations between *ISG20* expression and immune lymphocytes, chemokines, receptors, immunoinhibitors, immunostimulators, and major histocompatibility complex (MHC) molecules in almost cancer types assessed (Figures 7A–F).

3.8 CD increases *ISG20* expression in various cancer cell lines

Some small molecules or natural active components can affect gene expression. We wanted to determine whether small

molecules or natural components targeted *ISG20* expression. To do this, we first used the DrugBank database and revealed that UMP (DB03685) might target *ISG20* (Table 1; Supplementary Figures 2A, B). Then, several cancer-cell lines were cultured and treated with 0, 10, 20, or 40 μ M UMP for 24 h, and cells were collected for RNA extraction and RT-PCR. However, the results showed that UMP did not affect *ISG20* mRNA expression in A549 lung cancer cells, HeLa cervical cancer cells, 22RV1 and PC3 prostate cancer cells, and MDA-MB-231 and BT549 breast cancer cells (Supplementary Figures 2C–H).

Then, CD, a nucleoside derivative, was applied to determine the effect on *ISG20* expression in the cancer cell lines. The results showed that CD increased *ISG20* expression at both the protein and mRNA level in a dose-dependent manner in the H1975 lung cancer-cell line (Figures 8A, B) and 22RV1 prostate cancer-cell line (Figures 8C, D).

3.9 m^6_2A increases *ISG20* expression in HepG2 cancer cells

The effects of m^6_2A , another nucleoside derivative, on *ISG20* expression in cancer cell lines were also determined. Our results showed that m^6_2A increased *ISG20* expression at both the

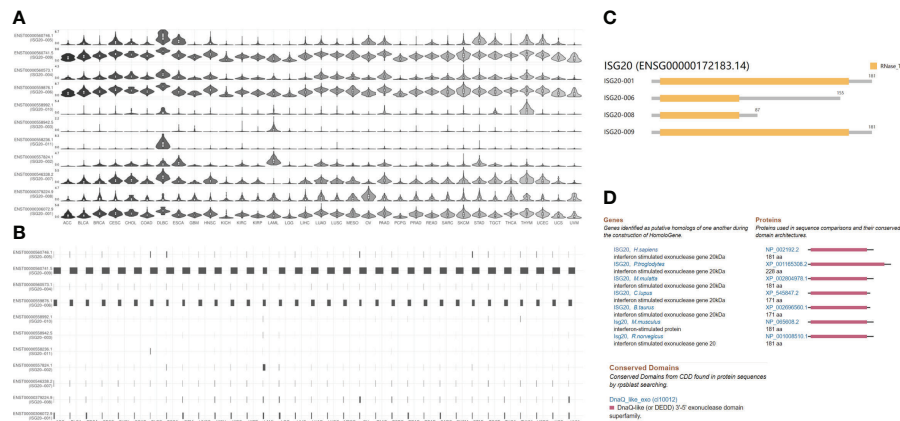


FIGURE 5

ISG20 isoform expression distribution, utilization, structure in pan-cancer, and conservation of ISG20 across different species. (A) The expression profiles of the ISG20 isoforms (violin plot). (B) Utilization profiles of the ISG20 isoforms (bar plot). (C) Structure of the ISG20 isoforms in pan-cancer. Information on 7 isoforms is missing; specifically, ENST00000546338.2, ENST00000557824.1, ENST00000558236.1, ENST00000558942.5, ENST00000558992.1, ENST00000560573.1, and ENST00000560746.1. (D) Conservation of ISG20 across different species.

protein and mRNA level in a dose-dependent manner in the HepG2 liver cancer cell line (Figures 8E, F).

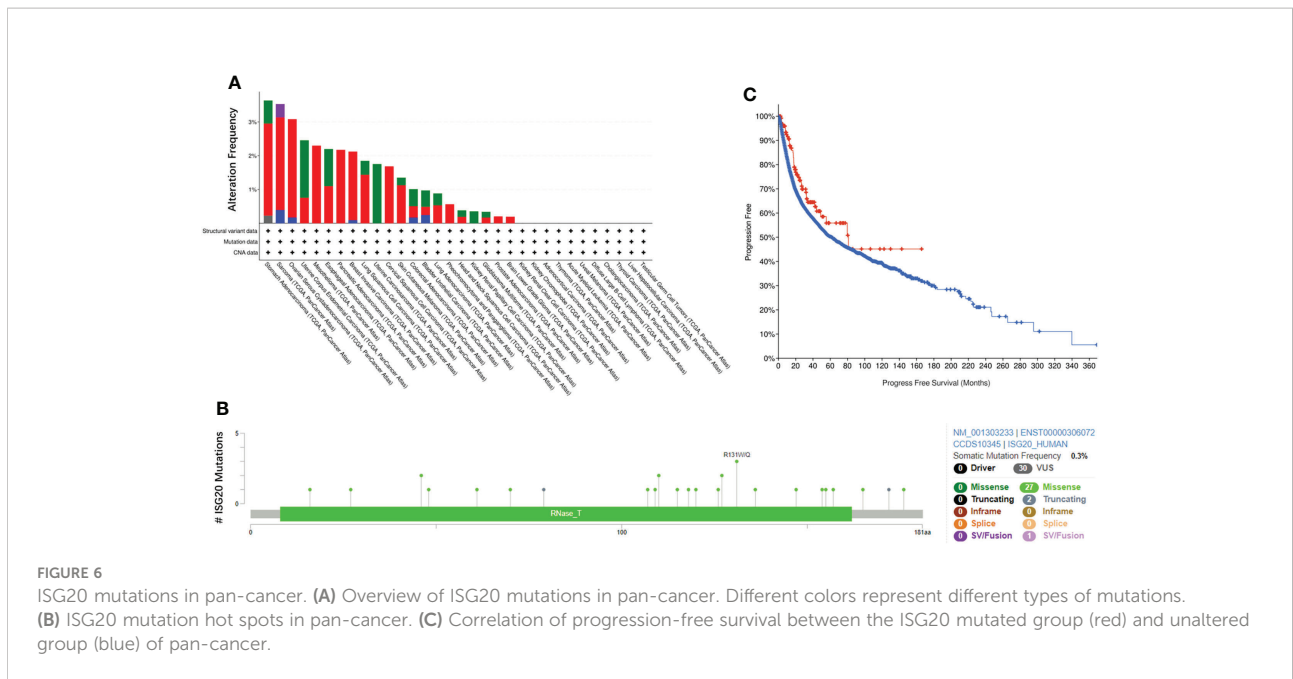
Altogether, both nucleoside derivatives, CD and m^6_2A , are predicted to exhibit antiviral/anti-SARS-CoV-2 therapeutic potential by increasing ISG20 expression.

4 Discussion

In this study, we found that the *ISG20* mRNA was primarily located in the bone marrow and lymphoid tissues; interestingly, the *ISG20* mRNA expression levels were significantly increased in 11 different types of cancer, including ACC, CESC, DLBC, GBM, KIRC, KIRP, LIHC, PAAD, SKCM, TGCT, and UCEC; and no decreases were observed in any type of cancer. Among these, higher expression of *ISG20* was associated with a longer OS in CESC and SKCM, suggesting that *ISG20* may be a good marker in both viral prevention and cancer progression in patients with these types of cancer. Unlike other receptors, such as ACE2, TMPRSS4, and CTSL, increased *ISG20* expression may prevent viral invasion in these types of cancer. DNA methylation is known to affect gene expression, and we found that *ISG20* promoter methylation was significantly lower in BLCA, READ, and THCA tumor tissues compared with those in the matched normal tissues, while higher in BRCA, LUSC, KIRC, and PAAD. Hypermethylation of *ISG20* in KIRC and PAAD tumor tissues was correlated with the higher expression, suggesting that methylation of *ISG20* may not underlie the increase in its expression; thus, other mechanisms may be involved in

regulating *ISG20* overexpression. Interestingly, both CD and m^6_2A increase *ISG20* expression in various cancer cell lines, even though it is unknown whether CD and m^6_2A regulate *ISG20* expression by modification of DNA methylation patterns. Due to the indispensability of antiviral processes and anti-tumor responses in the immune system, the correlation between *ISG20* expression and immune infiltration levels of pan-cancer was analyzed, and we revealed significant correlations between *ISG20* expression and immune lymphocytes, chemokine, receptors, immunoinhibitors, immunostimulators, and MHC molecules in all cancer types, highlighting a potential antiviral/anti-SARS-CoV-2 role.

Certain small molecules or natural active components can affect gene expression. We first performed DrugBank database searches and revealed *ISG20* as a UMP target. UMP was demonstrated to possess an anti-fibrillatory effect by activating energy metabolism (32). Unfortunately, our experiments failed to find UMP-regulated *ISG20* expression in cancer cells. We, therefore, further tested whether CD and m^6_2A could affect *ISG20* expression and found that both promoted *ISG20* expression at the protein and mRNA levels. CD is a natural active component of traditional Chinese medicine (TCM) fungus *cordyceps militaris*, which has anticancer properties (33–35). m^6_2A is a modified ribonucleoside in the tRNA of *mycobacterium bovis*, according to Bacille Calmette-Guérin (36). CD and m^6_2A are nucleoside derivatives that have been reported to inhibit the expression of CTSL, another SARS-CoV-2 receptor, in cancer cell lines (26). In addition, CD inhibited the expression of furin, another SARS-CoV-2 receptor, in several cancer cell lines (17). As CTSL inhibitors, both CD and m^6_2A can promote *ISG20*



upregulation. Considering ISG20 inhibits viral replication and/or degradation, CD and m⁶A may play roles in preventing SARS-CoV-2 invasion and the severity of cancer.

Altogether, our study revealed the expression and distribution patterns of ISG20 in virus/SARS-CoV-2 invasion

inhibition on different tissues and organs, differential expression and methylation patterns, and the prognostic significance across several types of cancer. ISG20 can play an important role in SARS-CoV-2 inhibition in certain types of cancer. Although future studies are needed for validation, our current study

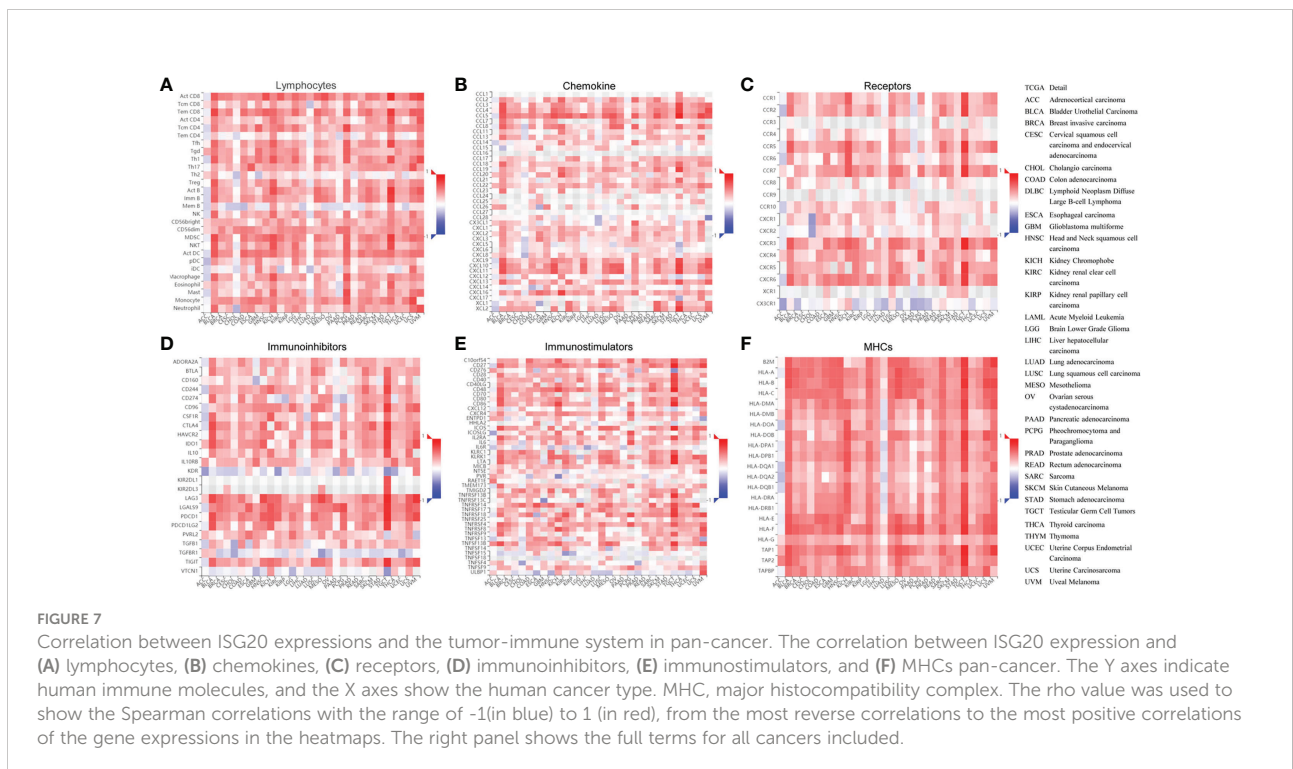
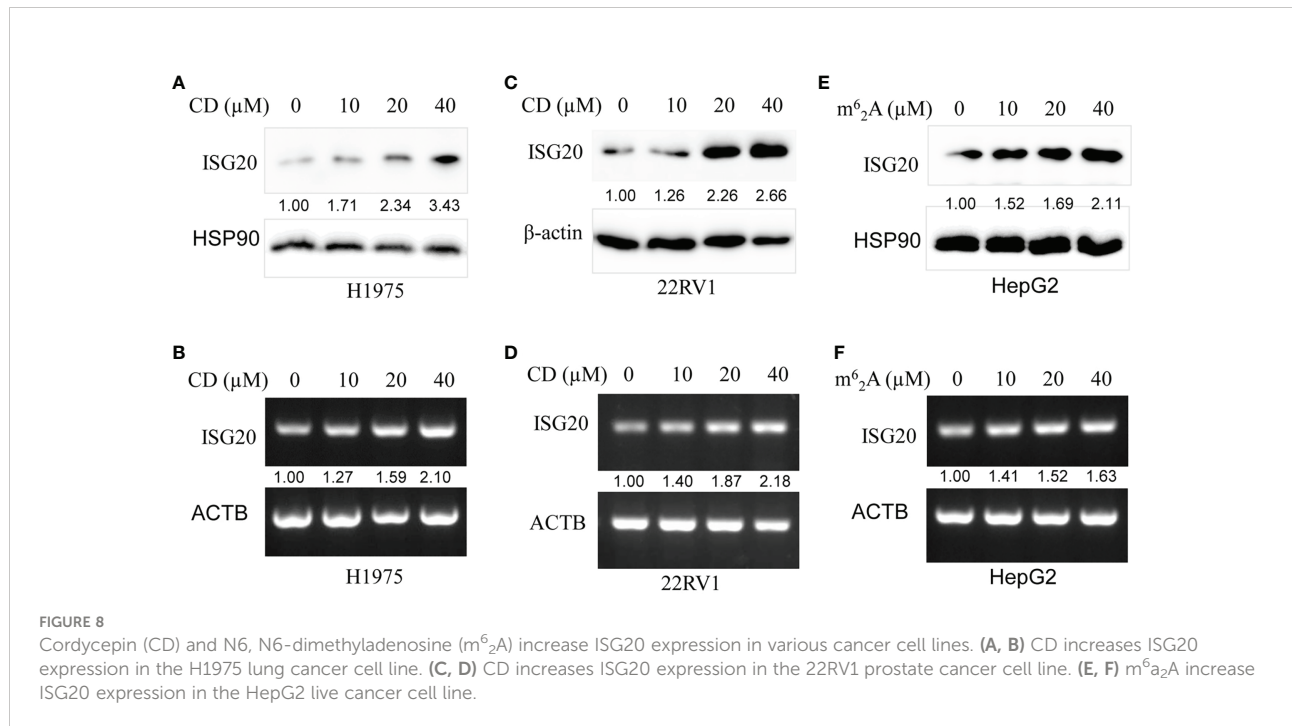


TABLE 1 Drugs predicted to target ISG20.

Drug ID	Name	Drug type	Predicted targets	Target no.
DB03685	Uridine monophosphate	Small Molecule	B4GALT1, GLT6D1, ISG20, LSM6, UCKL1	5



provides useful information to understand the current COVID-19 pandemic better. Moreover, small molecules from TCM or natural products may be used in the development of anti-SARS-CoV-2 drugs as well anticancer agents by upregulating ISG20 expression. Our study highlighted the value of targeting ISG20 as an alternative therapeutic strategy in combating cancer, SARS-CoV2, and other viral-caused diseases such as HAV, HBV, HCV, IAV, YFV, and BTV.

Data availability statement

The original contributions presented in the study are included in the article/[Supplementary Material](#). Further inquiries can be directed to the corresponding authors.

Ethics statement

This study was reviewed and approved by The study was approved by the Ethical Committee of Southwest Medical University and The Affiliated Huaian No. 1 People's Hospital

of Nanjing Medical University. The patients/participants provided their written informed consent to participate in this study.

Author contributions

JC, QT, JWF, ZL, XL, KG, LZ, JH, BZ, DL performed experimental studies, data acquisition, data analysis, and literature search. JJF collected and analyzed the data. JJF wrote and edited the manuscript. JJF, JC, DL revised the manuscript. All authors contributed to the article and approved the submitted version.

Funding

This work was supported by the Foundation of Science and Technology Department of Sichuan Province (grant no. 2022NSFSC0737), the Foundation of Southwest Medical University (grant nos. 2021ZKMS004, 2021ZKQN109), in part by the Research Foundation of Luzhou City (grant no. 2021-

SYF-37), and the National Natural Science Foundation of China (grant nos. 81672887 and 82073263).

Acknowledgments

The authors thank all the people from the Research Center for Preclinical Medicine, Southwest Medical University.

Conflict of interest

The authors declare that the research was conducted in the absence of any commercial or financial relationships that could be construed as a potential conflict of interest.

References

- Gongora C, David G, Pintard L, Tissot C, Hua TD, Dejean A, et al. Molecular cloning of a new interferon-induced PML nuclear body-associated protein. *J Biol Chem* (1997) 272:19457–63. doi: 10.1074/jbc.272.31.19457
- Pentecost BT. Expression and estrogen regulation of the HEM45 mRNA in human tumor lines and in the rat uterus. *J Steroid Biochem Mol Biol* (1998) 64:25–33. doi: 10.1016/S0960-0760(97)00140-4
- Deymier S, Louvat C, Fiorini F, Cimarelli A. ISG20: An enigmatic antiviral RNase targeting multiple viruses. *FEBS Open Bio* (2022) 12:1096–111. doi: 10.1002/2211-5463.13382
- Qu H, Li J, Yang L, Sun L, Liu W, He H. Influenza a virus-induced expression of ISG20 inhibits viral replication by interacting with nucleoprotein. *Virus Genes* (2016) 52:759–67. doi: 10.1007/s11262-016-1366-2
- Wu N, Nguyen XN, Wang L, Appourchaux R, Zhang C, Panthu B, et al. The interferon stimulated gene 20 protein (ISG20) is an innate defense antiviral factor that discriminates self versus non-self translation. *PLoS Pathog* (2019) 15:e1008093. doi: 10.1371/journal.ppat.1008093
- Stadler D, Kachele M, Jones AN, Hess J, Urban C, Schneider J, et al. Interferon-induced degradation of the persistent hepatitis b virus cccDNA form depends on ISG20. *EMBO Rep* (2021) 22:e49568. doi: 10.15252/embr.201949568
- Weiss CM, Trobaugh DW, Sun C, Lucas TM, Diamond MS, Ryman KD, et al. The interferon-induced exonuclease ISG20 exerts antiviral activity through upregulation of type I interferon response proteins. *mSphere* (2018) 3:e00209–18. doi: 10.1128/mSphere.00209-18
- Kang D, Gao S, Tian Z, Zhang G, Guan G, Liu G, et al. ISG20 inhibits bluetongue virus replication. *Viral Sin* (2022) 37(4):521–30. doi: 10.1016/j.virs.2022.04.010
- Chen X, Sun D, Dong S, Zhai H, Kong N, Zheng H, et al. Host interferon-stimulated gene 20 inhibits pseudorabies virus proliferation. *Viral Sin* (2021) 36:1027–35. doi: 10.1007/s12250-021-00380-0
- Ye G, Liu H, Zhou Q, Liu X, Huang L, Weng C. A tug of war: Pseudorabies virus and host antiviral innate immunity. *Viruses* (2022) 14:547. doi: 10.3390/v14030547
- Furutani Y, Toguchi M, Higuchi S, Yanaka K, Gailhouse L, Qin XY, et al. Establishment of a rapid detection system for ISG20-dependent SARS-CoV-2 subreplicon RNA degradation induced by interferon-alpha. *Int J Mol Sci* (2021) 22:11641. doi: 10.3390/ijms22111641
- Elkrief A, Hennessy C, Kuderer NM, Rubinstein SM, Wulff-Burchfield E, Rosovsky RP, et al. Geriatric risk factors for serious COVID-19 outcomes among older adults with cancer: A cohort study from the COVID-19 and cancer consortium. *Lancet Healthy Longev* (2022) 3:e143–52. doi: 10.1016/S2666-7568(22)00009-5
- Desai A, Gupta R, Advani S, Ouellette L, Kuderer NM, Lyman GH, et al. Mortality in hospitalized patients with cancer and coronavirus disease 2019: A systematic review and meta-analysis of cohort studies. *Cancer* (2021) 127:1459–68. doi: 10.1002/cncr.33386

Publisher's note

All claims expressed in this article are solely those of the authors and do not necessarily represent those of their affiliated organizations, or those of the publisher, the editors and the reviewers. Any product that may be evaluated in this article, or claim that may be made by its manufacturer, is not guaranteed or endorsed by the publisher.

Supplementary material

The Supplementary Material for this article can be found online at: <https://www.frontiersin.org/articles/10.3389/fimmu.2022.958898/full#supplementary-material>

- Grivas P, Khaki AR, Wise-Draper TM, French B, Hennessy C, Hsu CY, et al. Association of clinical factors and recent anticancer therapy with COVID-19 severity among patients with cancer: a report from the COVID-19 and cancer consortium. *Ann Oncol* (2021) 32:787–800. doi: 10.1016/j.annonc.2021.02.024
- Fu C, Stoeckle JH, Masri L, Pandey A, Cao M, Littman D, et al. COVID-19 outcomes in hospitalized patients with active cancer: Experiences from a major new York city health care system. *Cancer* (2021) 127:3466–75. doi: 10.1002/cncr.33657
- Fu J, Liao L, Balaji KS, Wei C, Kim J, Peng J. Epigenetic modification and a role for the E3 ligase RNF40 in cancer development and metastasis. *Oncogene* (2021) 40:465–74. doi: 10.1038/s41388-020-01556-w
- Li D, Liu X, Zhang L, He J, Chen X, Liu S, et al. COVID-19 disease and malignant cancers: The impact for the furin gene expression in susceptibility to SARS-CoV-2. *Int J Biol Sci* (2021) 17:3954–67. doi: 10.7150/ijbs.63072
- Uhlen M, Fagerberg L, Hallstrom BM, Lindskog C, Oksvold P, Mardinoglu A, et al. Proteomics. Tissue-based map of the human proteome. *Science* (2015) 347:1260419. doi: 10.1126/science.1260419
- Uhlen M, Zhang C, Lee S, Sjoestedt E, Fagerberg L, Bidkhori G, et al. A pathology atlas of the human cancer transcriptome. *Science* (2017) 357(6352):eaan2507. doi: 10.1126/science.aan2507
- Tang Z, Li C, Kang B, Gao G, Li C, Zhang Z. GEPIA: a web server for cancer and normal gene expression profiling and interactive analyses. *Nucleic Acids Res* (2017) 45:W98–W102. doi: 10.1093/nar/gkx247
- Tang Z, Kang B, Li C, Chen T, Zhang Z. GEPIA2: an enhanced web server for large-scale expression profiling and interactive analysis. *Nucleic Acids Res* (2019) 47:W556–W60. doi: 10.1093/nar/gkz430
- Ding W, Chen J, Feng G, Chen G, Wu J, Guo Y, et al. DNMT3D: DNA methylation interactive visualization database. *Nucleic Acids Res* (2020) 48:D856–D62. doi: 10.1093/nar/gkz830
- Cerami E, Gao J, Dogrusoz U, Gross BE, Sumer SO, Aksoy BA, et al. The cBio cancer genomics portal: An open platform for exploring multidimensional cancer genomics data. *Cancer Discovery* (2012) 2:401–4. doi: 10.1158/2159-8290.CD-12-0095
- Ru B, Wong CN, Tong Y, Zhong JY, Zhong SSW, Wu WC, et al. TISIDB: An integrated repository portal for tumor-immune system interactions. *Bioinformatics* (2019) 35:4200–2. doi: 10.1093/bioinformatics/btz210
- Zhang L, Yang M, Gan L, He T, Xiao X, Stewart MD, et al. DLX4 upregulates TWIST and enhances tumor migration, invasion and metastasis. *Int J Biol Sci* (2012) 8:1178–87. doi: 10.7150/ijbs.4458
- Zhang L, Wei C, Li D, He J, Liu S, Deng H, et al. COVID-19 receptor and malignant cancers: Association of CTSL expression with susceptibility to SARS-CoV-2. *Int J Biol Sci* (2022) 18:2362–71. doi: 10.7150/ijbs.70172
- Wang K, Deng H, Song B, He J, Liu S, Fu J, et al. The correlation between immune invasion and SARS-CoV-2 entry protein ADAM17 in cancer patients by bioinformatic analysis. *Front Immunol* (2022) 13:923516. doi: 10.3389/fimmu.2022.923516

28. Fu J, Zhou B, Zhang L, Balaji KS, Wei C, Liu X, et al. Expressions and significances of the angiotensin-converting enzyme 2 gene, the receptor of SARS-CoV-2 for COVID-19. *Mol Biol Rep* (2020) 47:4383–92. doi: 10.1007/s11033-020-05478-4
29. Yu J, Liu TT, Liang LL, Liu J, Cai HQ, Zeng J, et al. Identification and validation of a novel glycolysis-related gene signature for predicting the prognosis in ovarian cancer. *Cancer Cell Int* (2021) 21:353. doi: 10.1186/s12935-021-02045-0
30. Blume C, Jackson CL, Spalluto CM, Legebeke J, Nazlamova L, Conforti F, et al. A novel ACE2 isoform is expressed in human respiratory epithelia and is upregulated in response to interferons and RNA respiratory virus infection. *Nat Genet* (2021) 53:205–14. doi: 10.1038/s41588-020-00759-x
31. Onabajo OO, Banday AR, Stanifer ML, Yan W, Obajemu A, Santer DM, et al. Interferons and viruses induce a novel truncated ACE2 isoform and not the full-length SARS-CoV-2 receptor. *Nat Genet* (2020) 52:1283–93. doi: 10.1038/s41588-020-00731-9
32. Bul'on VV, Krylova IB, Selina EN, Rodionova OM, Evdokimova NR, Saprionov NS, et al. Antiarrhythmic effect of uridine and uridine-5'-monophosphate in acute myocardial ischemia. *Bull Exp Biol Med* (2014) 157:728–31. doi: 10.1007/s10517-014-2653-3
33. Radhi M, Ashraf S, Lawrence S, Tranholm AA, Wellham PAD, Hafeez A, et al. A systematic review of the biological effects of cordycepin. *Molecules* (2021) 26(19):5886. doi: 10.3390/molecules26195886
34. Tima S, Tapingkae T, To-Anun C, Noireung P, Intaparn P, Chaiyana W, et al. Antileukaemic cell proliferation and cytotoxic activity of edible golden cordyceps (*Cordyceps militaris*) extracts. *Evid Based Complement Alternat Med* (2022) 2022:5347718. doi: 10.1155/2022/5347718
35. Wei C, Khan MA, Du J, Cheng J, Tania M, Leung EL, et al. Cordycepin inhibits triple-negative breast cancer cell migration and invasion by regulating EMT-TFs SLUG, TWIST1, SNAIL1, and ZEB1. *Front Oncol* (2022) 12:898583. doi: 10.3389/fonc.2022.898583
36. Chan CT, Chionh YH, Ho CH, Lim KS, Babu IR, Ang E, et al. Identification of N6,N6-dimethyladenosine in transfer RNA from *Mycobacterium bovis* bacille Calmette-Guérin. *Molecules* (2011) 16:5168–81. doi: 10.3390/molecules16065168